Spatiotemporal chaos in sine-Gordon systems subjected to wave fields: Onset and suppression

R. Chacón,[1] A. Bellorín,[2] L. E. Guerrero,[3] and J. A. González[4]

[1]*Departamento de Física Aplicada, Escuela de Ingenierías Industriales, Universidad de Extremadura, Apartado Postal 382, E-06071 Badajoz, Spain*

[2]*Escuela de Física, Facultad de Ciencias, Universidad Central de Venezuela, Apartado 47586, Caracas 1041-A, Venezuela*

[3]*Departamento de Física, Universidad Simón Bolívar, Apartado 89000, Caracas 1080-A, Venezuela*

[4]*Centro de Física, Instituto Venezolano de Investigaciones Científicas, Apartado 21827, Caracas 1020-A, Venezuela*

The onset of spatiotemporal chaos in a damped sine-Gordon system subjected to a plane wave field as well as its suppression by an additional small-amplitude plane wave field are proposed theoretically and confirmed numerically. The relevance of these findings in the context of nonlinear magnetization waves is discussed.

In the last decade, the problem of suppressing or enhancing spatiotemporal chaos has been the center of a great deal of attention and effort on the part of the scientific community, partly because of its many and diverse applications, including the stabilization of semiconductor laser arrays [1], superconducting Josephson-junction arrays [2], and periodic patterns in optical turbulence [3], and partly because it may be regarded as a first step toward the control of turbulence [4]. It seems especially interesting to consider this problem in the context of sine-Gordon (SG) systems [5] given the broad applicability of the SG equation, which describes propagation of magnetic flux in Josephson junctions [2], flux-line unlocking in type-II superconductors [6], propagation of ultrashort optical pulses in resonant laser media [7], motion of dislocations in crystals [8], and DNA dynamics [9], to cite just a few phenomena. With respect to previous work, suppression of temporal phase-locked chaos in a damped SG system in the presence of two ac (sinusoidal in time, homogeneous in space) excitations was demonstrated by numerical simulations in Ref. [10]. The present work considers a damped SG system subjected to two spatiotemporal fields in the form of monochromatic waves:

$$U_{tt} - U_{xx} + \sin U = -\alpha U_t + \Gamma \sin(\omega t - k_n x)$$
$$+ \eta\Gamma \sin(\Omega t - k'_n x - \Psi), \quad (1)$$

where the amplitudes Γ, $\eta\Gamma$, wave numbers $k_n \equiv 2\pi n/L$, $k'_n \equiv 2\pi n'/L$, and frequencies ω, Ω correspond to the chaos-inducing and chaos-suppressing fields, respectively, Ψ is the initial phase, L is the total length of the system, and one assumes weak dissipation $(0 < \alpha < 1)$ and small amplitudes $(0 < \eta, \Gamma < 1)$. Physically, Eq. (1) describes, for example, the dynamics of the orientation angle $U(x,t)$ of the magnetization vector lying in the easy plane of a quasi-one-dimensional easy-plane ferromagnet in the presence of a strong constant magnetic field **H** (lying in the easy plane) and two additional weak variable magnetic fields in the form of monochromatic waves, both being perpendicular to **H** [11–13]. In the absence of any chaos-suppressing field $(\eta = 0)$ and for $\exp[iU(x,t)] = \exp[iU(x+L,t)]$, $U(x,t=0) = U_t(x,t=0) = 0$, two different regimes characterized by the conditions $k_n < \omega$ and $k_n > \omega$, respectively, have been identified [14]. In this case, since periodic wave trains locked to

the wave field $\Gamma \sin(\omega t - k_n x)$ are observed numerically in both regimes (for certain ranges of the parameters), it is natural to consider an ansatz of the form $U(\omega t - k_n x)$ for the solutions of the complete SG equation (1) to study the effectiveness of the secondary wave field in suppressing the spatiotemporal chaos induced by the primary wave field. This is the well-known method of phase plane analysis [15], which is a general method for seeking traveling-wave solutions (see Ref. [15] and references therein for more details). Thus, with the additional imposition that the two waves have the same phase velocity, Eq. (1) reduces to the perturbed pendulum equations

$$u_{\zeta\zeta} + \sin u = \alpha'_1 u_\zeta + \Gamma \sin(W_1 \zeta) + \eta\Gamma \sin(W'_1 \zeta + \Theta), \quad (2)$$

for $k_n > \omega$, where $u \equiv U - \pi$, $W_1^2 \equiv k_n^2 - \omega^2 \equiv k_n^2(1 - v_f^2)$, $\zeta \equiv (\omega t - k_n x - \pi)/W_1$, $W'_1 \equiv \Omega W_1/\omega$, $\alpha'_1 \equiv \alpha\omega/W_1$, and

$$u_{\xi\xi} + \sin u = -\alpha'_2 u_\xi - \Gamma \sin(W_2 \xi) - \eta\Gamma \sin(W'_2 \xi + \Theta), \quad (3)$$

for $k_n < \omega$, where $W_2^2 \equiv \omega^2 - k_n^2 \equiv k_n^2(v_f^2 - 1)$, $\xi \equiv (\omega t - k_n x - \pi)/W_2$, $W'_2 \equiv \Omega W_2/\omega$, $\alpha'_2 \equiv \alpha\omega/W_2$, and where $\Theta \equiv \pi(\Omega/\omega - 1) - \Psi$, $v_f \equiv \omega/k_n = \Omega/k'_n$ are the common initial phase and phase velocity, respectively. When the absolute value of the phase velocity is sufficiently greater than unity, one sees that both equations satisfy the requirements of Melnikov's method (MM), i.e., $0 < \alpha'_{1,2} < 1$ [16,17]. One can therefore apply this method to obtain analytical estimates of the ranges of the parameters $(\eta, \Omega, k'_n, \Theta)$ for inhibition of the spatiotemporal chaos existing in the absence of the chaos-suppressing field. In particular, the application of MM to Eqs. (2) and (3) yields their respective Melnikov functions (MFs)

$$M^\pm(\zeta_0) = D_1 \pm A_1 \sin(W_1 \zeta_0) \pm B_1 \sin(W'_1 \zeta_0 + \Theta), \quad (4a)$$

$$M^\pm(\xi_0) = -D_2 \mp A_2 \sin(W_2 \xi_0) \mp B_2 \sin(W'_2 \xi_0 + \Theta), \quad (4b)$$

where $D_{1,2} \equiv 8\alpha'_{1,2}$, $A_{1,2} \equiv 2\pi\Gamma \,\text{sech}(\pi W_{1,2}/2)$, $B_{1,2} \equiv 2\pi\eta\Gamma \,\text{sech}[\pi\Omega W_{1,2}/(2\omega)]$, and where the plus (minus) sign of the MFs refers to the upper (lower) homoclinic orbit of the unperturbed pendulum. We assume in the following that, in the absence of any chaos-suppressing field $(\eta = 0)$,
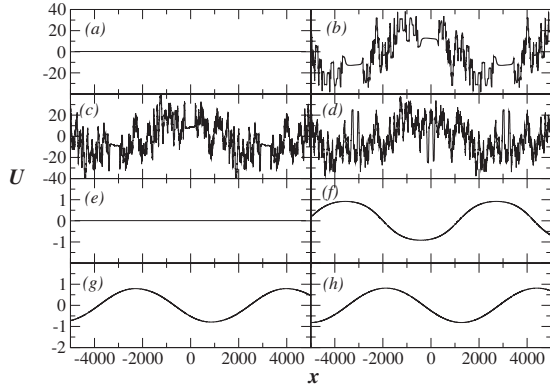
FIG. 1. Solution profiles for increasing time instants from $t=0$ (a),(e) in the absence (presence) of a chaos-suppressing field $\eta=0$ (a)–(d) [$\eta=0.5, \Psi=-\pi$, (e)–(h)]. Fixed parameters $L=10^4$, $\alpha=0.1$, $\Gamma=0.922$, $k_n=0.001$, $\omega=\Omega=0.6$.

the above perturbed pendulums exhibit homoclinic chaos which corresponds to spatiotemporal chaos existing in the SG system (1). The theoretical results on chaos suppression by weak periodic perturbations [18] now directly apply to the above MFs, and one straightforwardly obtains the three following predictions.

(i) Let $\Omega=p\omega$, where p is a positive integer, be such that $\Theta=\Theta_{\mathrm{opt}}^+=\Psi_{\mathrm{opt}}^+\equiv\pi,3\pi/2,0,\pi/2$, for $p=4n-3,4n-2,4n-1,4n$ ($n=1,2,\ldots$), respectively. Then $M^+(\zeta_0)$ and $M^+(\xi_0)$ always have the same sign (i.e., homoclinic chaos is suppressed) if and only if the following condition is satisfied:

$$\eta_{\mathrm{min}} < \eta \leq \eta_{\mathrm{max}}, \tag{5a}$$

$$\eta_{\mathrm{min}} \equiv (1 - D_{1,2}/A_{1,2})R_{1,2}, \tag{5b}$$

$$\eta_{\mathrm{max}} \equiv R_{1,2}/p^2, \tag{5c}$$

$$R_{1,2} \equiv \cosh(\pi p W_{1,2}/2)/\cosh(\pi W_{1,2}/2). \tag{5d}$$

(ii) Let $\Omega=p\omega$, where p is a positive integer, be such that $\Theta=\Theta_{\mathrm{opt}}^-=\Psi_{\mathrm{opt}}^-\equiv\pi,\pi/2,0,3\pi/2$, for $p=4n-3,4n-2,4n-1,4n$ ($n=1,2,\ldots$), respectively. Then $M^-(\zeta_0)$ and $M^-(\xi_0)$ always have the same sign (i.e., homoclinic chaos is suppressed) if and only if Eqs. (5a)–(5d) are satisfied [cf. Eqs. (4a) and (4b)].

(iii) For the main resonance case, $\Omega=\omega$, the MFs $M^\pm(\zeta_0)$ and $M^\pm(\xi_0)$ always have the same sign (i.e., homoclinic chaos is suppressed) inside the regions of the Ψ-η parameter plane limited by the boundary functions

$$\eta = -\cos\Psi \pm \sqrt{\cos^2\Psi - (1 - D_{1,2}^2/A_{1,2}^2)}. \tag{6}$$

We found that numerical experiments accurately confirmed the theoretical predictions. Figures 1 and 2 show two illustrative examples. Typically, one finds that complete regularization appears inside islands which *symmetrically* contain the theoretically predicted areas where even chaotic transients are suppressed (see Fig. 2).

Two remarks are now in order. First, in the absence of any chaos-suppressing field ($\eta=0$), the perturbed pendulums (2) and (3) can exhibit homoclinic chaos if
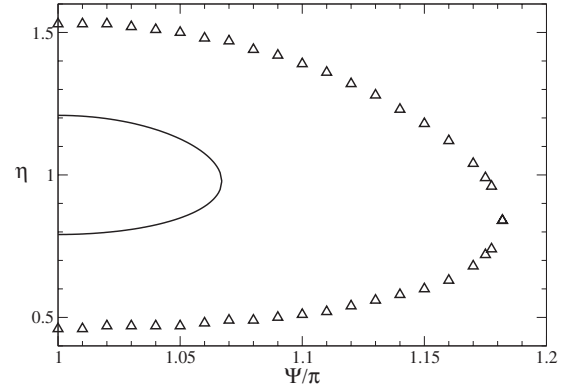
FIG. 2. Regularization region in the Ψ-η parameter plane for an initial situation of spatiotemporal chaos [Eq. (1)]. The solid black contour indicates the predicted boundary function [cf. Eq. (6)], while the triangle contour corresponds to the numerically obtained regularization region. Here $\Gamma=0.9$, and the remaining parameters are as in Fig. 1. Only results corresponding to the interval $\Psi\in[\pi,2\pi]$ are shown because of symmetry.

$$\frac{\Gamma}{\alpha} \geq F_1^{\mathrm{th}} \tag{7a}$$

and

$$\frac{\Gamma}{\alpha} \geq F_2^{\mathrm{th}}, \tag{7b}$$

respectively, where the chaotic threshold functions are given by

$$F_1^{\mathrm{th}} \equiv \frac{4v_f}{\pi}(1 - v_f^2)^{-1/2}\cosh\left(\frac{\pi k_n}{2}\sqrt{1 - v_f^2}\right), \tag{8a}$$

$$F_2^{\mathrm{th}} \equiv \frac{4v_f}{\pi}(v_f^2 - 1)^{-1/2}\cosh\left(\frac{\pi k_n}{2}\sqrt{v_f^2 - 1}\right). \tag{8b}$$

One straightforwardly obtains the limit $\lim_{v_f\to 1}F_i^{\mathrm{th}}=\infty$, $i=1,2$, i.e., in such a limit chaotic behavior is not possible. Also, for the limiting case of a purely temporal forcing, $k_n=0$, one has $\lim_{v_f\to\infty}F_2^{\mathrm{th}}=4\cosh(\pi\omega/2)/\pi\equiv F_2^{\mathrm{th}}(\omega)$, which is a monotonically increasing function of the driving frequency. Second, for each homoclinic orbit of the integrable pendulum, the optimal values for suppression, Θ_{opt} (and Ψ_{opt}), are the same for both regimes (i.e., $v_f>1$ and $v_f<1$), for each resonance order p.

To obtain additional insight into the onset of spatiotemporal chaos, consider the limiting case of a time-independent perturbation:

$$U_{tt} - U_{xx} + \sin U = -\alpha U_t + F(x), \tag{9}$$

where $F(x)$ is a periodic function having alternating maxima, zeros, and minima. It has been shown that the zeros of $F(x)$ are possible candidate equilibrium positions for kinks and antikinks, which could appear as a result of the dynamics described by Eq. (9). One has that the zeros x^* [$F(x^*)=0$] with $(\partial F/\partial x)_{x=x^*}>0$ are stable (unstable) equilibria for kinks (antikinks), and vice versa for the zeros satisfying
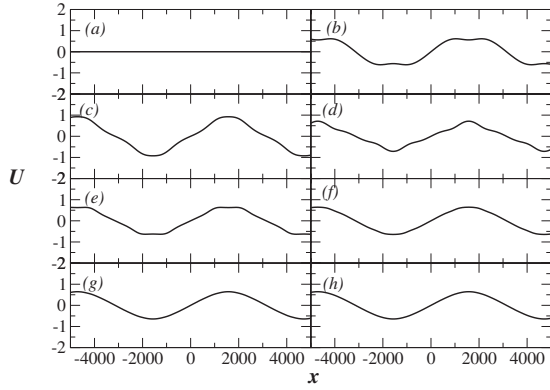
FIG. 3. Solution profiles for increasing time instants from $t=0$ (a) for $\eta=\omega=0$, and the remaining parameters as in Fig. 1. Notice that the asymptotic spatial structure is a (time-independent) attractor.

$(\partial F/\partial x)_{x=x^*}<0$ [19,20]. To be specific, let us choose

$$F(x) \equiv \frac{2(B^2-1)\sinh(Bx)}{\cosh^2(Bx)}, \qquad (10)$$

which has a unique zero at $x^*=0$. Stability analysis of the kink located at the equilibrium point leads to the following eigenvalue problem:

$$\hat{L}f(x) = \gamma f(x), \qquad (11)$$

where $\hat{L} \equiv -\partial_{xx} + \cos\phi_k(x)$, $\gamma \equiv -(\lambda^2+\alpha\lambda)$, and $\phi_k \equiv 4\arctan[\exp(Bx)]$ while $f(x)$ are the soliton modes describing small oscillations around the kink of the form $f(x)\exp(\lambda t)$. We found that the eigenvalues of the discrete spectrum are given by

$$\gamma_n = B^2(\Lambda + 2\Lambda n - n^2) - 1, \qquad (12)$$

with $\Lambda(\Lambda+1)=2/B^2$. One has that the amplitude of the perturbation can be increased by decreasing B, while the internal mode of the kink is unstable when $B^2 < (13-3\sqrt{17})/8$. This means that kinks can break up if they are close to an unstable equilibrium and the force's amplitude is sufficiently large. Also, the asymptotic behavior will be a stationary (time-independent) solution when the external force is purely spatial. However, the kink(s) will be subjected regularly to the presence of unstable equilibria in the case of a plane wave field [cf. Eq. (1)]. Note that approximating the extreme of the sinusoidal wave field profile with the function of Eq. (10) implies the conditions $\Gamma > 1-(13-3\sqrt{17})/8$ and $k_n < \sqrt{(13-3\sqrt{17})/8}$.

Extensive numerical experiments indicated that, if condition (7a) and (7b) is conjointly satisfied with the condition for the instability of the internal mode, turbulent behavior is typically observed, meaning that the solution is chaotic in both time and space, as in the example shown in Figs. 1(a)–1(d). When the dynamics is controlled by the secondary wave field ($\eta>0$), the solution is usually a periodic wave which moves at the same velocity as the driving field [see Fig. 1(e)–1(h)]. For $\omega=0$, Fig. 3 shows that the spatiotemporal dynamics tends to a stationary structure. This structure is
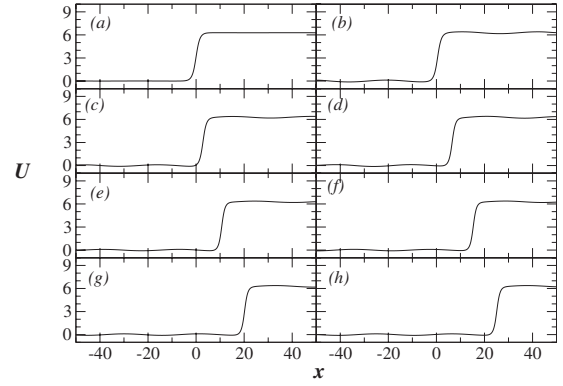
FIG. 4. Soliton profiles for different time instants [cf. Eq. (1); $L=100$, $\alpha=0.1$, $\Gamma=0.1$, $k_n=0.2$, $\omega=0.1$, $\eta=0$], showing that when the internal modes are stable and the phase velocity of the external field is below a certain threshold value, the kink can be transported by the external field.

an attractor of the SG system which plays a role similar to that of a fixed point in a purely temporal system. Since in the present case the system is spatiotemporal, such an attractor can be space dependent. Another important regime occurs when the equilibria of the "moving" periodic potential are such that the internal modes are stable. In such a case, a kink will be transported by the wave with its center of mass sitting at the bottom of one of the stable equilibria (see Fig. 4). The transport of kinks by an external wave field has recently been considered in Ref. [20]. However, if the velocity of the external wave field is sufficiently large, the kink cannot be carried by the field. An estimate for when this would first occur is

$$\frac{\omega}{k_n} > \frac{\Gamma}{\alpha}, \qquad (13)$$

which can be understood as follows. When the spatial periodic force $F(x)$ in Eq. (9) presents a single sign, the stable kinks and antikinks will move with a velocity that is proportional to its amplitude (say Γ) and inversely proportional to the damping coefficient α (cf. Refs. [20,21]), while the direction of the motion will depend on the force's sign. For the SG system subjected to a dc force Γ [22], one has the following formula for the kink velocity:

$$V_{\text{kink}} = \frac{\pi\Gamma}{4\alpha}\left[1 + \left(\frac{\pi\Gamma}{4\alpha}\right)^2\right]^{-1/2}. \qquad (14)$$

However, when the external perturbation is a plane wave (i.e., a moving periodic force that periodically changes its sign) with a phase velocity $(\omega/k_n) > V_{\text{kink}}$, the kinks and antikinks cannot be stably carried by the plane wave field [20]. The connection of these results with those from MM may be clarified by the following considerations. First, note that condition (7a) and (7b) can be satisfied in the limiting case $\omega \to 0$. Second, we found numerically that there is no chaos in this case (see Fig. 3). In fact, chaos does not appear even for $\omega \gtrsim 0$, but one typically observes again a wave solution locked to the external periodic field, both moving with the same velocity. We thus conclude that there must be a thresh-

old value for the phase velocity for spatiotemporal chaos to be observed, i.e., one needs conditions (7a), (7b), and (13) together with the instability of the internal modes.

In conclusion, we have shown that spatiotemporal chaos of a SG system perturbed by a wave field is a very complex phenomenon. Its description cannot be completely reduced to an effective pendulum equation. One needs more than temporal-chaos-related concepts. We found that a combination of concepts including homoclinic bifurcations and the stability theory of soliton modes (as well as the possibility of transport of spatiotemporal structures by the moving effective potential created by the external wave field) allowed us to characterize this phenomenon. Additionally, we found that the theory of chaos suppression by an additional periodic perturbation can also be successfully applied to the case of developing turbulence, reflecting the importance of underlying homoclinic events. We expect that the present approach can be useful to control the chaotic dynamics of nonlinear magnetization waves, including magnetic solitons [23]. In particular, the present results can be extended to the case of an arbitrary angle χ between the strong constant magnetic field **H** (lying in the easy plane) and the two additional weak variable magnetic fields in the form of monochromatic waves [11–13]. Our current work is aimed at exploring this case.

[1] E. Schöll, *Nonlinear Spatio-Temporal Dynamics and Chaos in Semiconductors* (Cambridge University Press, Cambridge, U.K., 2000).

[2] A. Barone and G. Paternó, *Physics and Applications of the Josephson Effect* (Wiley, New York, 1982).

[3] W. Lu, D. Yu, and R. G. Harrison, Phys. Rev. Lett. **76**, 3316 (1996).

[4] I. Aranson, H. Levine, and L. Tsimring, Phys. Rev. Lett. **72**, 2561 (1994).

[5] A. Scott, *Nonlinear Science. Emergence and Dynamics of Coherent Structures* (Oxford University Press, Oxford, 1999).

[6] C. Cattuto and F. Marchesoni, Phys. Rev. Lett. **79**, 5070 (1997).

[7] G. L. Lamb, Rev. Mod. Phys. **43**, 99 (1971).

[8] J. Frenkel and T. Kontorova, J. Phys. (USSR) **1**, 137 (1939).

[9] S. W. Englander, N. R. Kallenbach, A. J. Heeger, J. A. Krumhansl, and S. Litwin, Proc. Natl. Acad. Sci. U.S.A. **77**, 7222 (1980); M. Salerno, Phys. Rev. A **44**, 5292 (1991); L. V. Yakushevich, Q. Rev. Biophys. **26**, 201 (1993).

[10] G. Filatrella, G. Rotoli, and M. Salerno, Phys. Lett. A **178**, 81 (1993).

[11] Y. S. Kivshar and B. A. Malomed, Rev. Mod. Phys. **61**, 763 (1989); Rev. Mod. Phys. **63**, 211 (1991).

[12] A. M. Kosevich, B. A. Ivanov, and A. S. Kovalev, *Nonlinear Magnetization Waves. Dynamical and Topological Solitons* (Naukova Dumka, Kiev, 1983) (in Russian).

[13] I. L. Lyubchansky, V. L. Sobolev, and T. K. Soboleva, Fiz. Nizk. Temp. **13**, 1061 (1987) [Sov. J. Low Temp. Phys. **13**, 603 (1987)].

[14] D. Cai, A. R. Bishop, and A. Sánchez, Phys. Rev. E **48**, 1447 (1993).

[15] See, e.g., E. Infeld and G. Rowlands, *Nonlinear Waves, Solitons and Chaos* (Cambridge University Press, Cambridge, U.K., 1990), p. 145.

[16] J. Guckenheimer and P. J. Holmes, *Nonlinear Oscillations, Dynamical Systems, and Bifurcations of Vector Fields* (Springer, Berlin, 1983).

[17] S. Wiggings, *Global Bifurcations and Chaos* (Springer-Verlag, New York, 1988).

[18] R. Chacón, Phys. Lett. A **257**, 293 (1999); Phys. Rev. Lett. **86**, 1737 (2001); Europhys. Lett. **54**, 148 (2001); Eur. Phys. J. B **30**, 207 (2002); Philos. Trans. R. Soc. London, Ser. A **364**, 2335 (2006).

[19] J. A. González and J. A. Hołyst, Phys. Rev. B **45**, 10338 (1992); J. A. González, L. E. Guerrero, and A. Bellorín, Phys. Rev. E **54**, 1265 (1996); J. A. González, B. A. Mello, L. I. Reyes, and L. E. Guerrero, Phys. Rev. Lett. **80**, 1361 (1998); J. A. González, A. Bellorín, and L. E. Guerrero, Phys. Rev. E **65**, 065601(R) (2002); J. A. González, S. Cuenda, and A. Sánchez, *ibid.* **75**, 036611 (2007).

[20] J. A. González, A. Marcano, B. A. Mello, and L. Trujillo, Chaos, Solitons Fractals **28**, 804 (2006).

[21] D. W. McLaughlin and A. C. Scott, Phys. Rev. A **18**, 1652 (1978).

[22] J. A. González and J. A. Hołyst, Phys. Rev. B **35**, 3643 (1987).

[23] A. M. Kosevich, B. A. Ivanov, and A. S. Kovalev, Phys. Rep. **194**, 117 (1990).